저마하수 난류 끝단 소음 예측

장강욱[1], 고성룡[1], 서정희[1], 문영준[2*]

PREDICTION OF TURBULENCE TRAILING-EDGE NOISE AT LOW MACH NUMBERS

K.W. Chang, S.R. Koh, J.H. Seo and Y.J. Moon

The turbulence noise generated from blunt trailing-edge is numerically predicted by using the hydrodynamic/acoustic splitting method at the Reynolds number based on thickness of flat plate, Re_h=1000, and the freestream Mach number M_o=0.2. The turbulent flow field is simulated by incompressible large-eddy simulation and the acoustic field is predicted efficiently with the linearized perturbed compressible equations (LPCE) recently proposed by the authors. The turbulent flow characteristics are validated with the results of the previous experimental study and direct numerical simulation. The acoustic properties predicted from LPCE are compared with the solutions of analytical formulations.

Key Words: 난류끝단소음(Turbulence Trailing-Edge Noise), 유동/소음분리기법(Hydrodynamic/Acoustic Splitting Method), 비압축성 큰 에디모사(Incompressible Large-Eddy-Simulation), 선형요동압축방정식(Linearized Perturbed Compressible Eqs.), 저마하수공력소음(Low Mach Number Aeroacoustics)

1. Introduction

As one of the important airframe noise problems, turbulent broadband noise generated at the trailing-edge of a lifting surface continues to pose a computational challenge. Since the trailing-edge noise is mostly concerned at low Mach numbers, it is computationally considered more challenging. In this regard, the trailing-edge noise problem has been treated by several hybrid methods: for example, after solving the incompressible large eddy simulation (*i*LES) for spectral quantifications of turbulences, acoustic analogy solutions are then sought by Wang & Moin [1] and Manoha and et al. [2]. More recently, similar trailing-edge noise calculation has been conducted by Ewert and Schröder [3], pursuing more direct descriptions of acoustic generation and propagation by the acoustically perturbed equations (APE), a splitting method based on a compressible LES solver.

The present study pursues a different hybrid approach, based on a hydrodynamic/acoustic splitting method. The turbulent flow is computed by *i*LES, while the near field compressibility as well as the far field acoustics is calculated by the linearized perturbed compressible equations (LPCE) [4]. The LPCE is a modified version of the original PCE [5], which is found very suitable to the turbulent flow noise predictions at low Mach numbers. In the previous study [4], it was found that the hydrodynamic/acoustic splitting method is very subtle to the coupling effects between the hydrodynamic vortical field and the perturbed velocities. This coupling effect caused by the non-linear interaction terms in the split perturbed equations causes unwanted errors by which inconsistent, grid-dependent acoustic solutions may be yielded. In the LPCE formulation, the instabilities caused by such coupling effects are firmly suppressed so that grid-independent acoustic solutions are secured. By this *i*LES/LPCE approach with the grid system splitting technique (i.e.

1 고려대학교 대학원 기계공학과
2 고려대학교 기계공학과
* Corresponding author E-mail: yjmoon@korea.ac.kr

fine grid for the *i*LES and coarse grid for the LPCE computation), turbulent noise at low Mach numbers can be predicted very efficiently.

In the present study, the noise generated by the blunt trailing edge of a flat plate submitted to the turbulent boundary layer is numerically predicted using the *i*LES/LPCE splitting method. The Reynolds number based on the thickness of a flat plate is Re_h=1000 and free stream Mach number is M_o=0.2 in the acoustic noise prediction.

2. Computational Methodology

In the present study, a low Mach number hydrodynamic field is solved by the incompressible large eddy simulation(*i*LES), while the compressible near field as well as the far field acoustics are computed by the linearized perturbed compressible equations with the acoustic source term, DP/Dt acquired during *i*LES computations. The governing equations for these two split methods are described below.

2.1 Incompressible Large Eddy Simulation(*i* LES)

The filtered incompressible Navier-Stokes equations can be written as,

$$\frac{\partial \overline{U_i}}{\partial x_i}=0 \tag{1}$$

$$\frac{\partial \overline{U_i}}{\partial t}+\frac{\partial \overline{U_i U_i}}{\partial x_j}=-\frac{1}{\rho_0}\frac{\partial \overline{P}}{\partial x_i}+\frac{\partial^2 \overline{U_i}}{\partial x_j \partial x_j}-\frac{\partial \tau_{ij}}{\partial x_j} \tag{2}$$

where $\tau_{ij}=\overline{U_i U_j}-\overline{U_i}\,\overline{U_j}$ is the subgrid-scale tensor and modeled as,

$$\tau_{ij}-\frac{1}{3}\delta_{ij}\tau_{kk}=-2C\overline{\Delta}^2\sqrt{2\overline{S_{ij}}\,\overline{S_{ij}}}\,\overline{S_{ij}} \tag{3}$$

where δ_{ij} is the Kronecker delta, $\overline{S_{ij}}$ is the filtered strain rate tensor, $\overline{\Delta}$ is the mean radius of a grid cell, i.e. the cubic root of its volume, and the model coefficient C is determined by dynamic SGS model [6].

For solving above filtered incompressible Navier-Stokes equations the fractional step method is employed and spatial derivatives are discretized using second-order central difference on a staggered mesh in Cartesian coordinates.

2.2 Linearized Perturbed Compressible Equations(LPCE)

In the hydrodynamic/acoustic splitting method, the total compressible flow variables are decomposed into the incompressible variables and the perturbed compressible flow variables as,

$$\begin{aligned}\rho(\vec{x},t)&=\rho_0+\rho'(\vec{x},t),\\ \vec{u}(\vec{x},t)&=\vec{U}(\vec{x},t)+\vec{u}'(\vec{x},t),\\ p(\vec{x},t)&=P(\vec{x},t)+p'(\vec{x},t)\end{aligned} \tag{4}$$

The perturbed quantities are computed by solving the linearized perturbed compressible equations (LPCE) [4] written as,

$$\frac{\partial \rho'}{\partial t}+(\vec{U}\cdot\nabla)\rho'+\rho_0(\nabla\cdot\vec{u}')=0, \tag{5}$$

$$\frac{\partial \vec{u}'}{\partial t}+(\vec{u}'\cdot\vec{U})+\frac{1}{\rho_0}\nabla p'=0, \tag{6}$$

$$\frac{\partial p'}{\partial t}+(\vec{U}\cdot\nabla)p'+\gamma P(\nabla\cdot\vec{u}')+(\vec{u}'\cdot\nabla)P=-\frac{DP}{Dt} \tag{7}$$

In contrast to the original PCE [5], the generation of perturbed vorticity is firmly suppressed in the LPCE formulation by dropping the coupled, second-order terms, in order to exclude errors caused by possible instability of perturbed vorticity. With this modification, the LPCE can now secure a 'grid-independent' acoustic solution at low Mach numbers (e.g. M_o=0.3), using the coarser acoustic grids and therefore its computational efficiency can considerably be improved. The perturbed compressible equations are spatially discretized by a sixth-order compact scheme and are temporally integrated using a fourth-order Runge-Kutta method.

3. Results and Discussions

3.1 *i*LES of Turbulent Flow past a Trailing-Edge

For the purpose of satisfying the statistical properties of turbulent boundary layer, a turbulence-inflow-generator proposed by Lund et al. [7] is used in the present LES computation. A computational domain for the flat-plate turbulent boundary layer(TBL) is $10\delta_0\times10\delta_0\times(\pi/3)\delta_0$ in the streamwise(x), wall-normal(y), spanwise(z) directions, respectively, where δ_0 is a mean turbulent boundary-layer thickness. The Reynolds number

based on the momentum thickness at the inlet boundary layer is $Re_\theta \cong 1220$. The computational meshes consist of 201×131×41 points in x, y, and z directions, having 100 points distributed in the y direction within 2 δ_0. The minimum computational grids are $\Delta x^+ \cong 25$, $\Delta y^+ \cong 0.9$, and $\Delta z^+ \cong 12.5$ in wall units.

The incompressible LES computation of the trailing-edge flow is performed by employing the flat-plate TBL solutions as an inflow condition. The computational domain for the trailing-edge is 126.5h×200h×10h in x, y and z directions, respectively, where h is the blunt trailing-edge thickness. The Reynolds number of the TBL at the trailing-edge is $Re_\theta \cong 1350$(or $Re_\tau = 540$). The TBL thickness at the trailing-edge corresponds to $\theta/h = 1.4$(or $\delta/h = 12.5$). The computational mesh consists of 213×311×41 points and the minimum computational grids are $\Delta x^+ \cong 2$, $\Delta y^+ \cong 0.9$, and $\Delta z^+ \cong 12.5$ in wall units.

The structure of turbulent eddies near the trailing edge is exhibited in Fig. 1. In Fig. 2, the wall pressure spectrum of turbulent boundary layer is compared with other DNS and experimental data and it is convinced that the spectral characteristics of wall turbulence are well resolved by present *i*LES calculation. Figure 3 shows the stream wise variation of the wall pressure spectra. The shape of spectrum is slightly changed at the trailing edge due to 'edge-effect' and the 'hump'caused by the bluntness of trailing edge is observed at Strouhal number fh/U_o=0.1.

3.2 LPCE Acoustic Computation of Turbulent Trailing-Edge Noise

Since the spanwise-dependency of coherent large eddy structure is little, the acoustic source is averaged over spanwise direction and the two-dimensional acoustic field computation is carried out. The computational domain for LPCE is extended to 200h in x-direction and has 301×301 points. A minimum acoustic grid size in the y direction is five times that of the hydrodynamic grid and the computational efficiency is achieved for this low Mach number aeroacoustic problem.

Figure 4 shows the acoustic source term DP/Dt field and it is observed that the most intense noise sources are distributed near the trailing edge. The instantaneous acoustic field computed by LPCE is presented in Fig. 5. The dipole characteristics of the noise generated by the turbulent eddy scattering at the trailing edge, is clearly visible. The power spectral densities of acoustic pressure at the far-field are shown in Fig. 6. The solid line is the result of present LPCE calculation and, for the purpose of comparison, the radiated acoustic pressure is also predicted using the analytical formulation proposed by Casper & Farassat (dotted line). Since the LPCE is computed on the two-dimensional domain, the monitored acoustic pressure is corrected to take into account a three-dimensional radiation effect. According to Oberai[8], the acoustic pressure radiated two-dimensionally, can be converted to the three-dimensionally radiated one using the approximated relation:

$$\Delta\tilde{p}'_{3D}(w) \simeq \Delta\tilde{p}'_{2D}(w) \cdot \frac{1+i}{2}\sqrt{\frac{w/c_0}{\pi r}} \tag{8}$$

The analytical formulation of Casper & Farassat (Formulation 1B[9]) is given by;

$$4\pi \cdot \Delta p'(\vec{x},t) = \int_S \left[\frac{(\partial P/\partial\tau + U_o \partial P/\partial x)(\hat{r}\cdot\hat{n})/|\vec{r}|}{c_o|\vec{r}| + c_o M_o(\vec{r}\cdot\hat{s})}\right]_{ret} dS + \int_S \left[\frac{P(\hat{r}\cdot\hat{n})/|\vec{r}|}{|\vec{r}|^2 + |\vec{r}| M_o(\vec{r}\cdot\hat{s})}\right]_{ret} dS - \int_\Omega \left[\frac{M_o P(\hat{r}\cdot\hat{n})^2/|\vec{r}|^2}{|\vec{r}| + M_o(\vec{r}\cdot\hat{s})}\right]_{ret} dl \tag{9}$$

where, $P(\vec{y},\tau)$ is the surface pressure obtained by present *i*LES computation, $\vec{x}$ is the observer position, $\vec{r}=\vec{x}-\vec{y}$, $\hat{n}$ and $\hat{s}$ are surface normal and parallel unit vectors, and S indicates the source surface and Ω is its boundary line. The subscript 'ret' denotes evaluation at retarded time $t-|\vec{r}|/c_0$. In this study, the source region is the upper surface of a flat plate near the trailing edge and integration is taken over $-5h \le x < 0$, $0 \le z \le 10h$. The observer position is at $\vec{x}=(0, 199h, 5h)$. Although a little discrepancy between the LPCE and analytical prediction is observed due to the fact that the only surface pressure is considered for the analytical prediction, the overall shape of spectra is comparably well met with.

5. Conclusions

The present LES results show a good agreement with the physical characteristics of turbulent boundary layer. The turbulence scales are directly influenced by the edge-effect. The frequency spectrum of wall pressure fluctuations is altered from w^{-1} to w^{-2} at the trailing-edge. A hybrid noise prediction method using LES & LPCE shows consistency with the result of *Howe*'s prediction model. Speculated primary noise source is the

near-wall spanwise vorticity mostly in the viscous-layer & buffer-layer at ω^+<0.4-0.5.

References

[1] Wang, M., and Moin, P., 2000, "Computation of Trailing-Edge Flow and Noise Using Large-Eddy Simulation," *AIAA Journal*, vol.38-12, pp.2201-2209.

[2] Manoha, E., Troff, B., and Sagaut, P., 2000, "Trailing-Edge Noise Prediction Using Large-Eddy Simulation and Acoustic Analogy," *AIAA Journal*, vol.38-4, pp.575-583.

[3] Ewert, R., and Schröder, W., 2004, "On the Simulation of Trailing Edge Noise with a Hybrid LES/APE Method," *Journal of Sound and Vibration*, vol.270, pp.509-524.

[4] Seo, J.H., and Moon, Y.J., 2005, "The Linearized Perturbed Compressible Equations for Aeroacoustic Noise Prediction at Very Low Mach Number," *11th AIAA/CEAS Aeroacoustics Conference*, Monterey, AIAA paper 2005-2927.

[5] Seo, J.H., and Moon, Y.J., 2005, "The Perturbed Compressible Equations for Aeroacoustic Noise Prediction at Low Mach Numbers," *AIAA Journal (in press)*.

[6] Germano, M., Piomelli, U., Moin, P., and Cabot, W.H., 1991, "A Dynamic Subgrid-Scale Eddy Viscosity Model," *Physics of Fluids*, vol.A3-7, pp.1760-1765.

[7] Lund, T. S., Wu, X., and Squires, K.D., 1998, "Generation of Turbulent Inflow Data for Spatially-Developing Boundary Layer Simulations," *Journal of Computational Physics*, vol.140, pp.233-258.

[8] Oberai, A.A., Roknaldin, F., and Hughes, T.J.R., 2002, " Trailing-Edge Noise due to Turbulent Flows," *Technical Report*, Boston University, Report No.02-002.

[9] Casper, J., and Farassat, F., 2004, "Broadband Trailing Edge Noise Predictions in the Time Domain," *Journal of Sound and Vibration*, vol.271, pp.159-176.

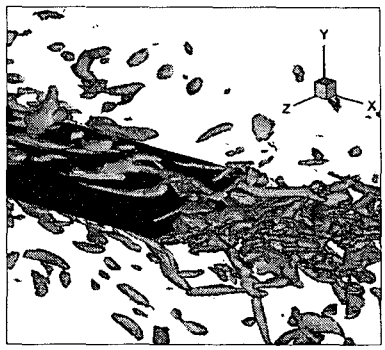

Fig. 1 Turbulent eddies at the trailing edge(Q=0.5).

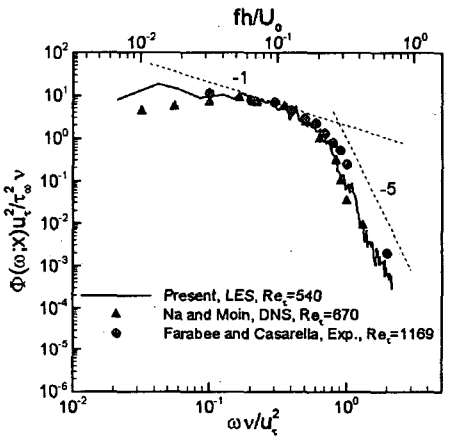

Fig. 2 Wall pressure fluctuation PSD scaled by inner variables.

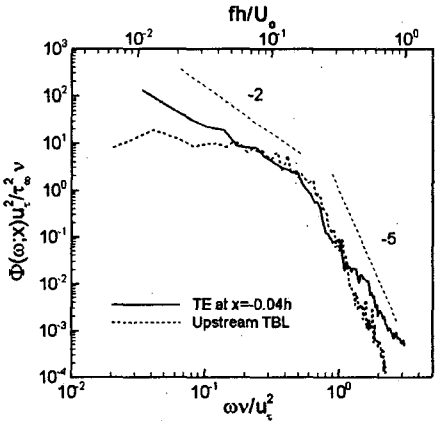

Fig. 3 Wall pressure fluctuation PSD at different locations.

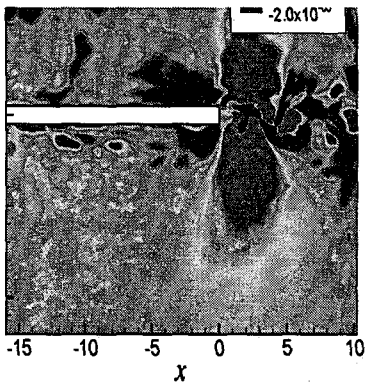

Fig. 4 Instantaneous trailing-edge noise sources beneath the TBL (DP/Dt field).

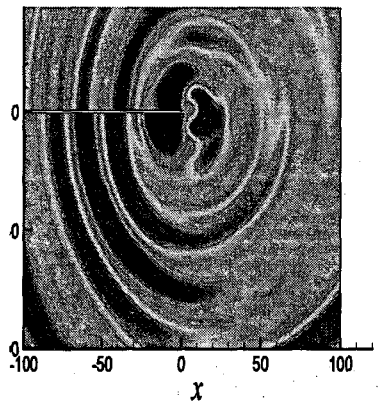

Fig. 5 Instantaneous acoustic field generated from the trailing edge.

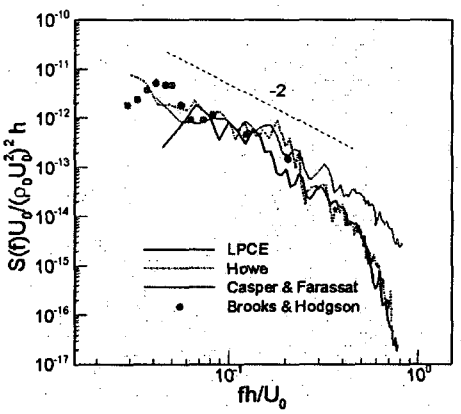

Fig. 6 Comparison of far field acoustic PSD at r=100h.